Electronic Supplementary Material (ESI) for Journal of Materials Chemistry B.

Supplementary Information

New features of edge-selectively hydroxylated graphene nanosheets as NIR-II photothermal agent and sonothermal agent for tumor therapy†

Wenqian Zhang, ‡[a] Man Fan, ‡[a] Ruchao Yang,[a] Zhihao Li,[a] Yuzhi Qiu,[a] Mengna Dong,[a] Peng Song,[a] Nan Wang,[a] Yajiang Yang[ab] and Qin Wang*[abc]

[a.] *Hubei Key Laboratory of Bioinorganic Chemistry and Materia Medica, School of Chemistry and Chemical Engineering, Huazhong University of Science and Technology, Wuhan, 430074, China. E-mail: qwang@hust.edu.cn*

[b.] *National Engineering Research Center for Nanomedicine, Wuhan 430074, China*

[c.] *Key Laboratory of Material Chemistry for Energy Conversion and Storage (Huazhong University of Science & Technology), Ministry of Education, Wuhan, 430074, China*

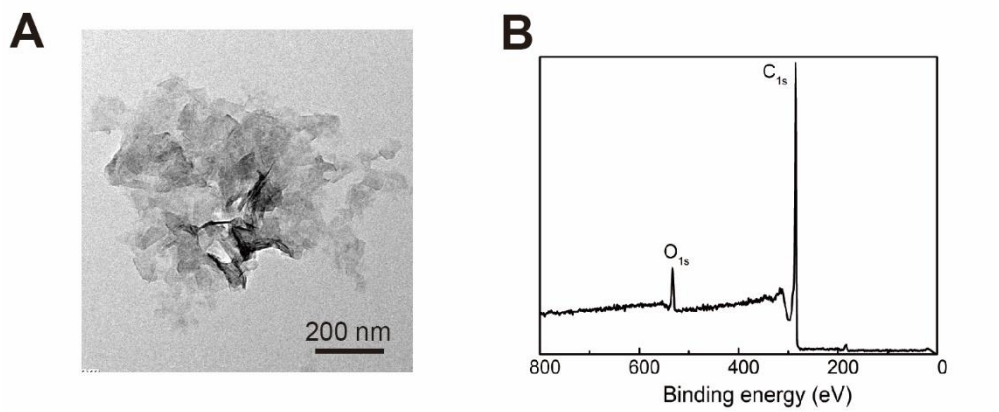

Fig. S1. (A) SEM image of the E2. (B) XPS spectrum of the E1.

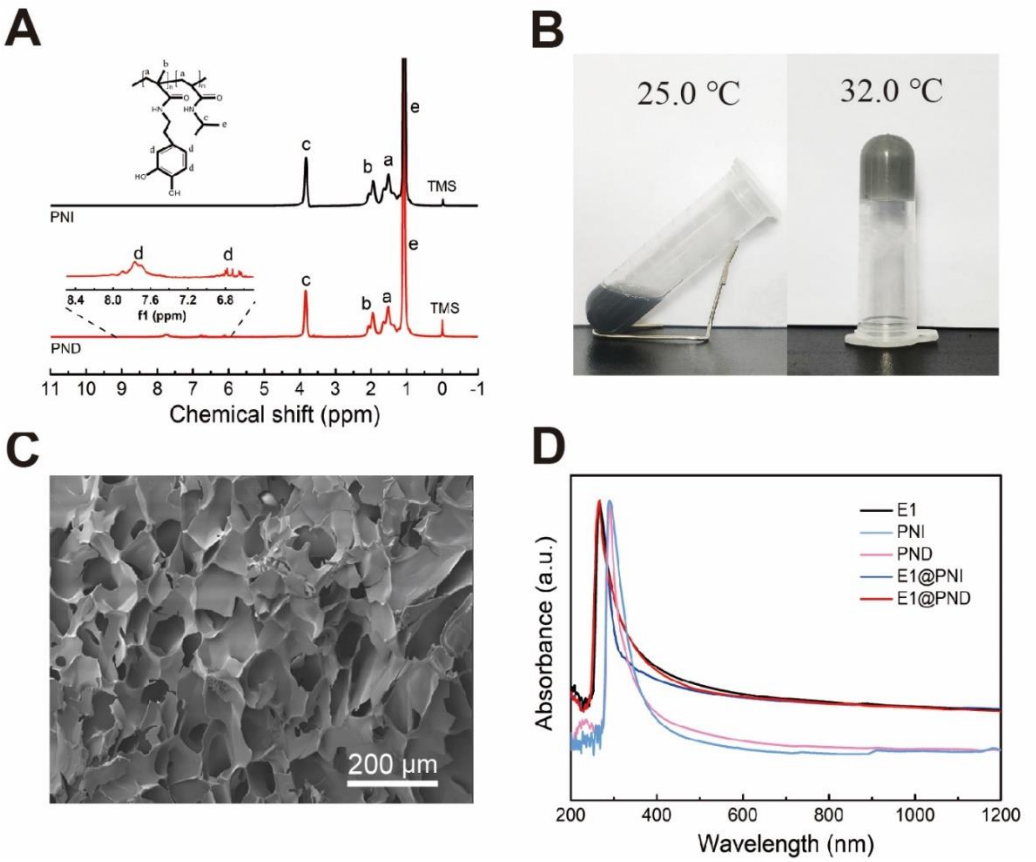

Fig. S2. (A) ^{1}H NMR spectra of the PND and PNI nanogels. (B) Photos showing a sol-gel phase transition of the injectable E1@PNI hydrogel. (C) SEM image of the forming PND hydrogel. (D) Normalized UV-Vis-NIR spectra of the E1, PNI, PND, E1@PNI and E1@PND dispersion.

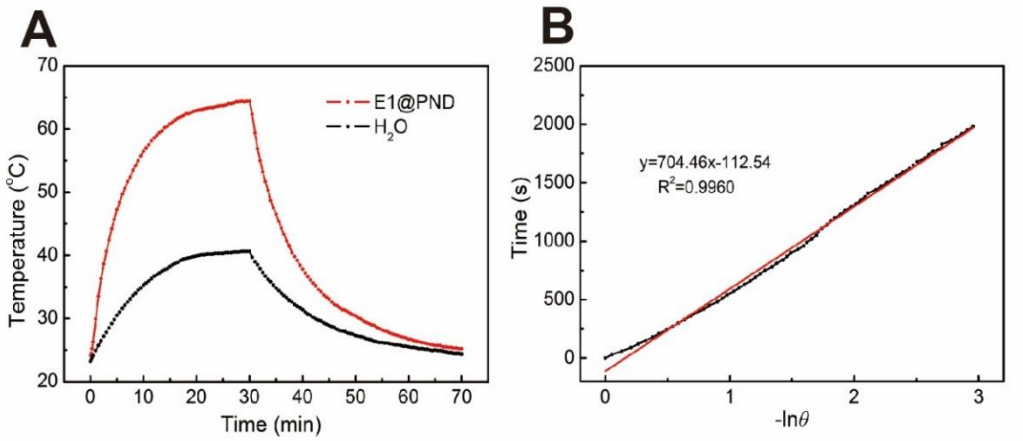

Fig. S3. Photothermal conversion efficiency of the injectable E1@PND hydrogel. (A) Heating and cooling curve. (B) Plots of time *versus* -lnθ based on Fig. S3A.

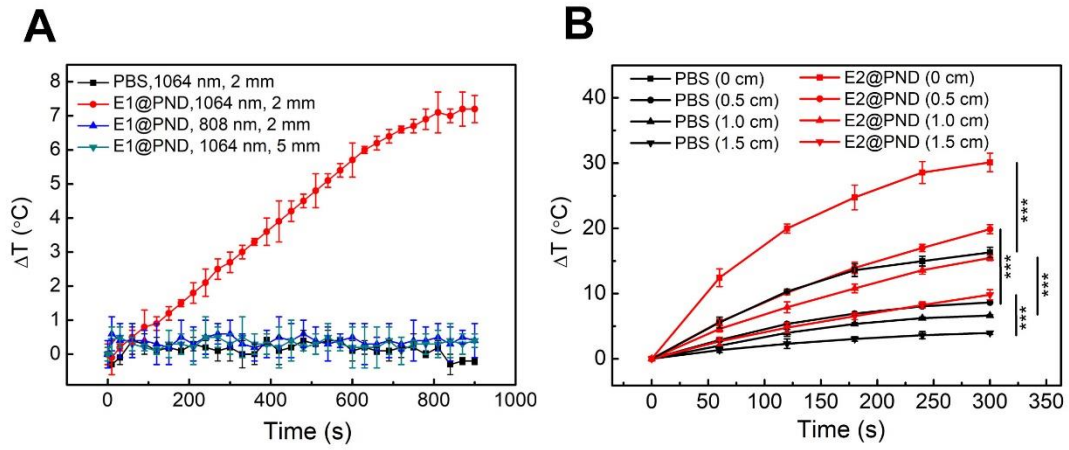

Fig. S4. (A) Photothermal performances of the injectable E1@PND hydrogel covered by chicken breast tissue with different thickness under 1064 and 808 nm laser irradiation (1.0 W cm^{-2}), respectively. (B) Sonothermal performances of the injectable E2@PND hydrogel covered by pork tissue with different thickness under ultrasound exposure (3.0 MHz, 1.8 W cm^{-2}, 60% duty cycle).

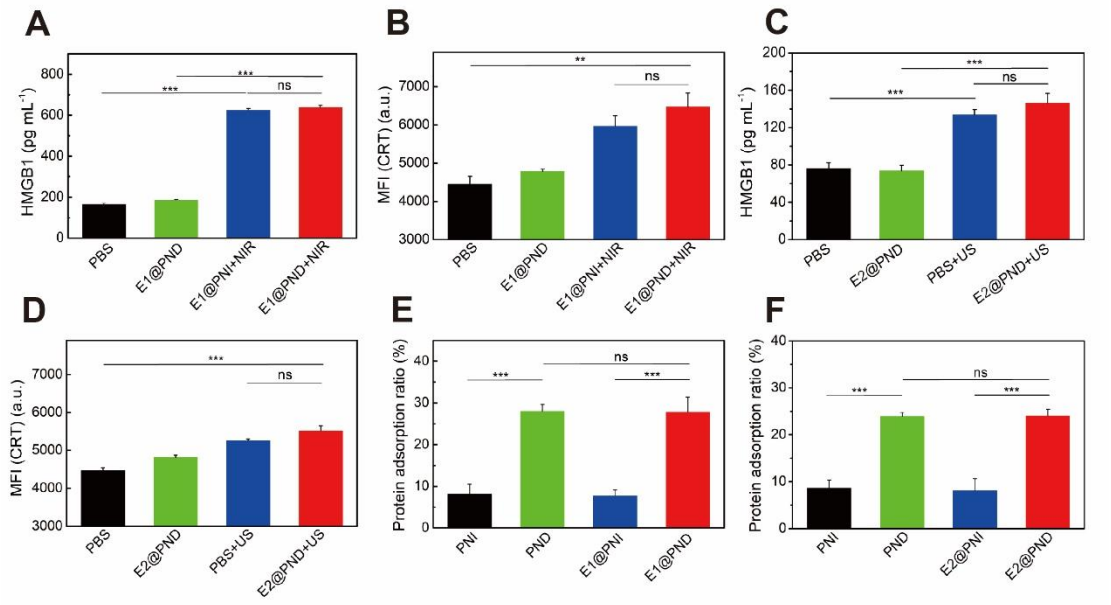

Fig. S5. Changes of ICD markers induced by NIR-II PTT and STT based on the injectable EHG@PND hydrogel. (A, C) Extracellular release amount of HMGB1 from 4T1 cells after various treatments (n=3). (B, D) CRT exposure on 4T1 cells after various treatments (n=3). (E-F) Protein adsorption ratio of the E1@PND and E2@PND hydrogels, respectively.

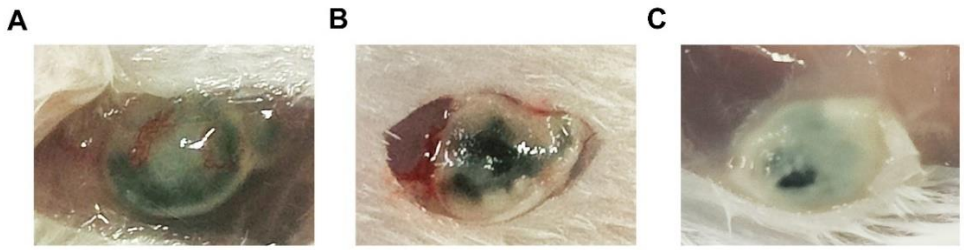

Fig. S6. Photos of the injectable E2@PND hydrogel at different times after subcutaneous injection. (A) Day 1. (B) Day 4. (C) Day 7.

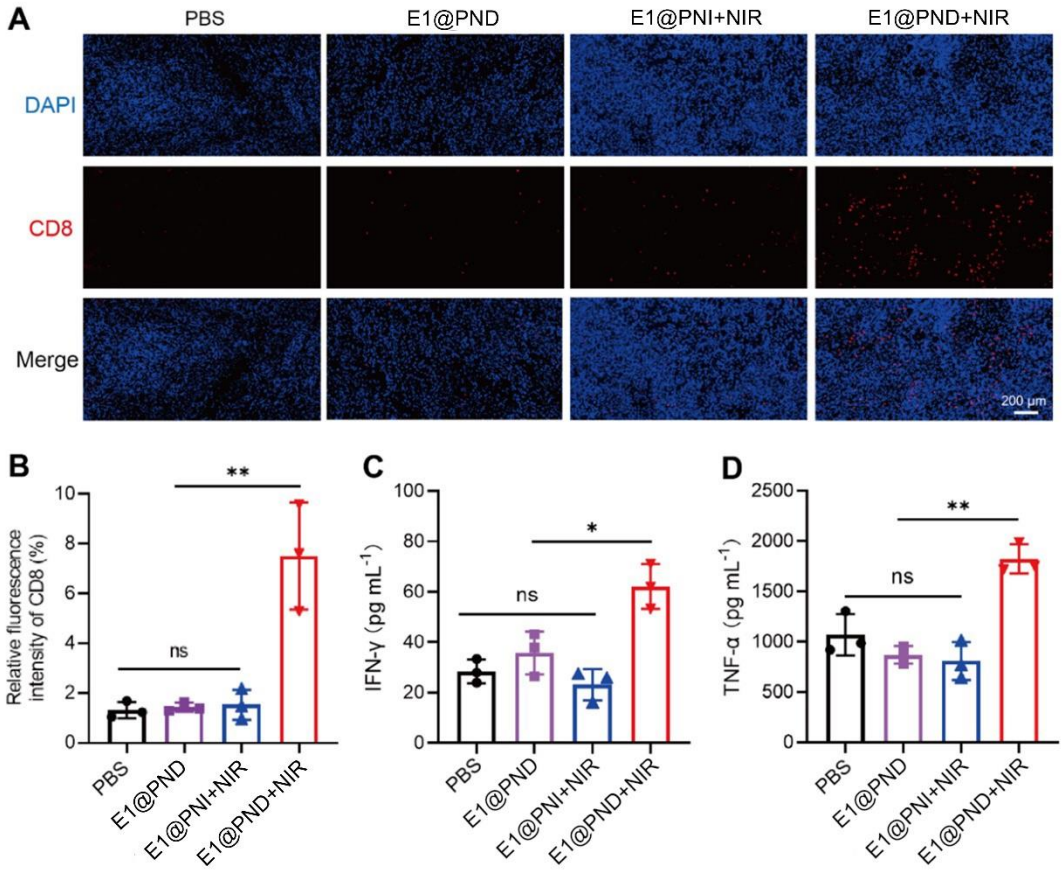

Fig. S7. Immune activation effects of the injectable E1@PND hydrogel-based PTT in the bilateral tumor experiments on day 8 post the first NIR-II laser irradiation. (A) Representative CD8 immunofluorescence staining images of the distal tumor tissues. (B) Quantitative statistical analysis of the CD8 level based on the immunofluorescence intensity (*n*=3). (C) IFN-*γ* level in mice sera (*n*=3). (D) TNF-*α* level in mice sera (*n*=3).

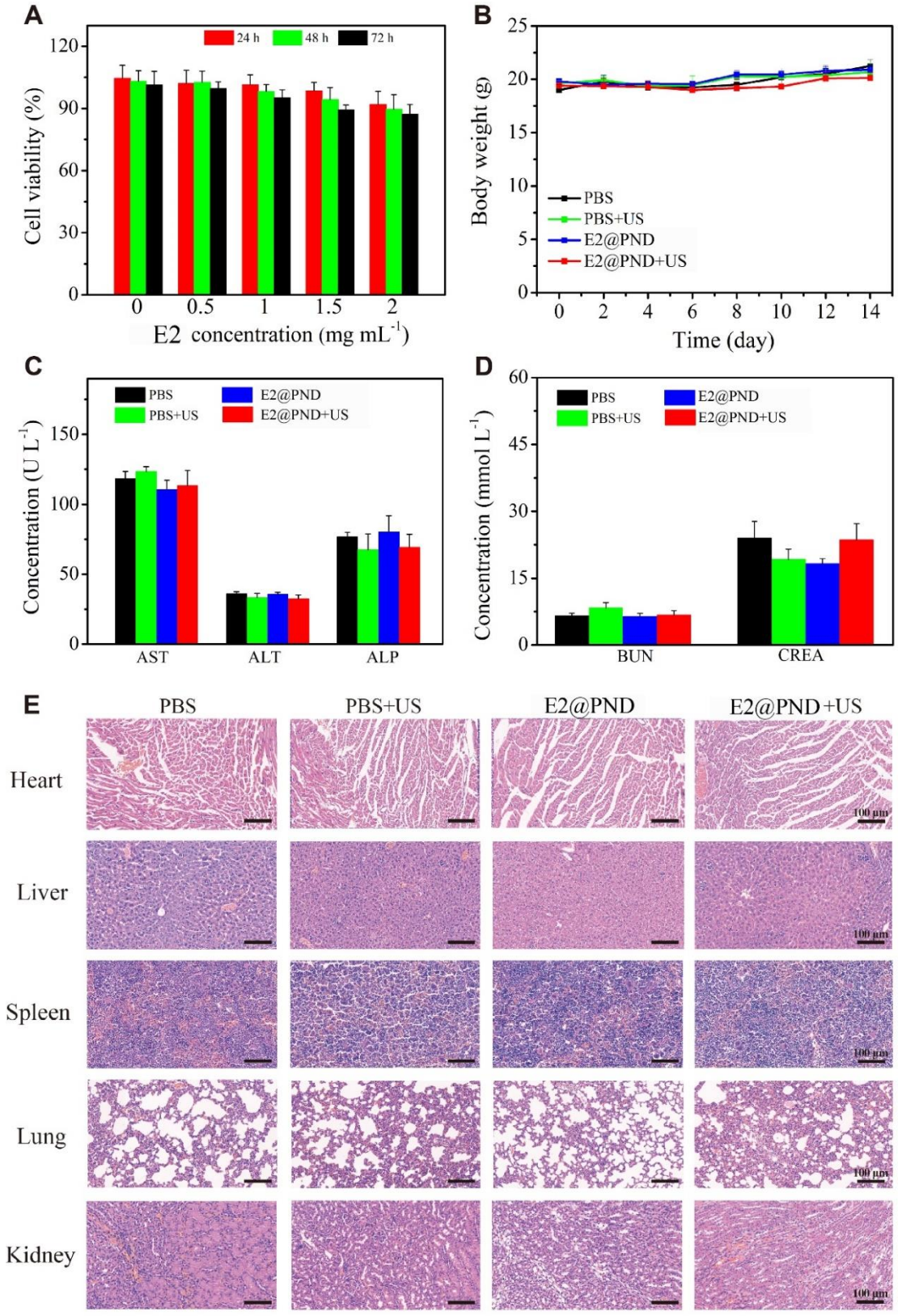

Fig. S8. Biosafety of the injectable E2@PND hydrogel-based STT. (A) Viability of HUVECs after co-incubation with the injectable E2@PND hydrogel containing various

amount of the E2 for 24 h, 48 h and 72 h, respectively (*n*=4). (B) Body weight changes of 4T1-bearing mice during the STT treatment (*n*=4). (C, D) Blood biochemistry analysis (AST, ALT, ALP, BUN, and CREA) of tumor-bearing mice treated by E2@PND-based STT. The sera are collected on day 14 after the first STT (*n*=3). (E) H&E staining images of the heart, liver, spleen, lung, and kidney of mice on day 14 after the first STT.